The geodynamics of Mt. Etna volcano during and after the 1984 eruption

Santo La Delfa ([1]), **Giuseppe Patanè** ([1]) **and Concetta Centamore** ([2])
([1]) *Istituto di Geologia e Geofisica, Università di Catania, Italy*
([2]) *Dipartimento di Geofisica e Vulcanologia, Università di Napoli «Federico II», Napoli, Italy*

Abstract
Data concerning $M > 2.5$ earthquakes that occurred at Mt. Etna volcano (Sicily, Italy) during the period April 15th - October 29th, 1984 are here presented and discussed. Only those events with reliable focal mechanisms (at least eight polarities) have been considered. Instrumental information comes from local seismic networks run by the University of Catania and the CNRS (Grenoble, France). The results obtained support the hypothesis that the seismicity and the volcanic activity at Mt. Etna are related to a complex stress field, due to the combined effects of the tectonics associated with the interaction between the African and Eurasian plates and the movement of magma into the crust. In particular, we hypothesize that the tectonic forces caused the end of the 1984 eruption, by means of a «locking mechanism».

Key words *Mt. Etna – earthquakes – focal mechanisms – stress field – eruption*

1. Introduction

Mt. Etna volcano is located between two main tectonic structures: the Iblean Foreland and the Northern Chain (or Apenninic-Maghrebian Chain). The former corresponds to the northern margin of the African plate, while the latter consists of a series of overthrust bodies, made up of sedimentary terranes deposited in the past along the African continental margin. Between the early Miocene and the Quaternary, in fact, the stratigraphic structural units of the chain, originated in various sedimentary basins, overlapped the more external domain (Lentini *et al.*, 1994).

At present the stress field acting on the Etnean area is due to the physical factors which caused this migration, the local stress fields produced by rising magma and the gravitative seaward sliding of the eastern sector of the volcano (Patanè *et al.*, 1994).

In the past, the stress field both by Oriental Sicily and by the Etnean area, was prevalently determined by African and Euroasiatic plate convergence.

The local seismicity and the different patterns of eruptive activity at summit craters of Mt. Etna seem to be strongly influenced by the reciprocal interaction among all the above factors.

The instrumental analysis of seismic activity at Mt. Etna started about thirty years ago; on the basis of observations made since 1971 it can be concluded that the Etnean earthquakes occur without significant temporal gaps, with swarms preceding and/or following the eruptions (Bottari *et al.*, 1975; Cosentino *et al.*, 1979, 1981; Glot *et al.*, 1984; Patanè *et al.*, 1984, 1986, 1994; Ferrucci *et al.*, 1993).

In particular, a detailed analysis of seismic activity at Mt. Etna during and after the eruption of April-October 1984 (Gresta *et al.*, 1987) discloses the complexity of the interaction among

Mailing address: Prof. Giuseppe Patanè, Istituto di Geologia e Geofisica, Università di Catania, Corso Italia 55, 95129 Catania , Italy; e-mail: patane@alp9ct.infn.it

the various structural trends in the Etnean area and the eruptive activity of the volcano.

Patanè *et al.* (1996) subsequently showed that the evolution formality of the 1991-1993 eruption was controlled both by fracture framework and by variations of local tensional field. In fact, volcanic phenomena which developed in two phases, separated by a brief temporal pause, accounted for the lack of manifestations.

The onset of the eruption (December 14th, 1991) was linked to a extensional stress field; after a momentary stop (about 24 h), bound by a compressive stress field, a shallow inflation (December 15th, 1991) drove the restart of the eruption, along a NNW-SSE fracture located in the western side of the «Valle del Bove».

The presence of other seismic data relative to the period April 27th - October 29th, 1984 allows us analyse the correlation between eruptive and seismic phenomena during and after the 1984 eruption at SE crater; more specifically, our observations concern the role of the stress field acting on the volcano in the above mentioned period.

2. Instrumental features

The seismic data analysed in this paper were collected by both the permanent network of Catania University and the temporary ARGOS network of IRIGM of Grenoble (fig. 1). Seismic stations of Catania University network were equipped with short period vertical seismometers (1 Hz). Seismic signals of the seven stations were centralized to the Earth Science Institute in Catania, by means of radio transmissions or phone lines. Seismic activity was continuously monitored both on charts and on magnetic tape.

The ten ARGOS stations were equipped with short period vertical seismometers (2 Hz), each of then including an analogical P-Picker with its ARGOS interface, and an ARGOS transmitter with its antenna.

Each detected event is characterized by: time of P arrival, width of the first half-wave (in hundredths of second), polarity of the first motion and quality of the reading. For more technical details see Glot *et al.* (1984).

3. Data analysis

Seismic activity with $M > 2.5$ located prevalently in the upper part of Etna between April 15th and October 29th 1984 has been considered for the present investigations.

More than 2400 local earthquakes were recorded, but we have considered only 103 fault plane solutions of the best located events (tables I and II).

Hypocentral computation was undertaken using a modified version of the HYPO71 program (Lee and Lahr, 1975), and the velocity model proposed for the region by Hirn *et al.* (1991).

The hypocentre of the earthquakes with $H \leq 10$ km has uncertainties (ERH, ERZ) within 3 km, for both the horizontal and vertical axes, while RMS ≤ 0.3 s. The earthquakes with $H > 10$ km show ERH, ERZ ≤ 4.0 km and RMS ≤ 0.3 s.

Figure 2 shows the epicentral distribution of earthquakes from April 15th to October 15th, 1984. The northeastern sector of the volcano is not directly involved during the eruption at SE crater (April 27th - October 16th), because most of the seismic events are concentrated in the upper part of the volcano and on the western side at intermediate and low altitudes.

As confirmed by analogous observations regarding other Etnean seismic events (Scarpa *et al.*, 1983; Glot *et al.*, 1984; Patanè *et al.*, 1984) the depths of hypocentres seem to be distributed mainly in two different intervals, respectively above and below a reference level at about 7 km b.s.l. (fig. 3a,b); it can be noticed, however, that the number of events concerning the deeper interval is smaller and their focii cluster mostly in the western sector of the volcano. Figure 4 reports focal mechanisms of the events whose locations are enumerated in fig. 5; one of the two focal planes, generally, have trend similar to those of the fault and fracture systems affecting the analysed sectors (fig. 6) and show prevalently NNE-SSW, NNW-SSE and NE-SW trends, while only a few have different orientations. Fault planes of shallower earthquakes ($H < 7$ km) show more dispersed trends, even if the NNE-SSW, NNW-SSE and NW-SE directions seem to be prevalent (see also table I);

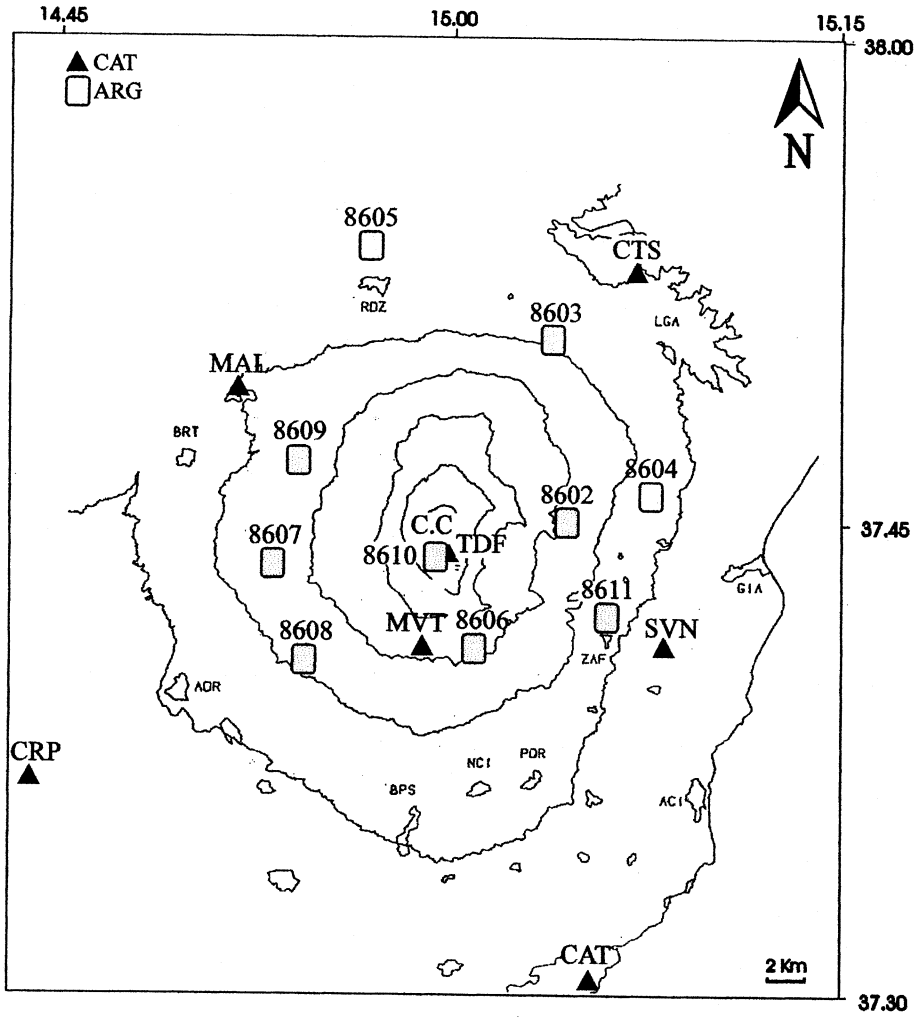

Fig. 1. Map of seismic networks (Catania University = triangles, Grenoble IRIGM = squares) operating at Mt. Etna in 1984; CC = Central Craters.

similarly (fig. 7a) a considerable dispersion is evident for the *P* axes of these events. On the contrary, *P* poles of deeper earthquakes are distributed mainly along the WNW-ESE trend (fig. 7b).

The epicentral map of seismic events from October 16th to 29th (fig. 8) points out that most of them are located in the upper part of the central-eastern sector of the volcano; in particular, seismic activity is more intense at intermediate-high altitudes and on the NW rim of «Valle del Bove», whereas only sporadic earthquakes are placed near its northern rim and at low altitudes of both western and eastern sectors of the volcano.

Figure 9a,b reports the hypocentres of events which occurred during post-eruptive seismic crisis; in agreement with previous observations, focii are prevalently clustered at shallower levels.

Table I. Focal parameters of earthquakes during the eruption. ERH = standard error on epicentre (km); ERZ = standard error on hypocentre (km); RMS = root mean square error of time residuals (s); GAP = maximum angle

No.	Date	h:min (GMT)	Origin	Long(°)	Lat(°)	Depth (km)	ERH	ERZ	RMS	GAP
1	15/04/84	3.10	44.42	14-53.64	37-37.25	3.18	1.1	1.7	0.29	147
2	04/06/84	22.52	19.57	14-58.57	37-40.85	11.36	2.2	2.9	0.30	168
3	04/06/84	22.54	31.57	14-59.07	37-40.70	12.63	1.1	1.5	0.16	171
4	04/06/84	22.56	45.51	14-57.77	37-40.10	1.32	0.9	1.3	0.17	110
5	04/06/84	22.58	2.42	14-57.46	37-42.70	4.97	2.7	2.2	0.15	89
6	04/06/84	23.10	37.78	14-58.14	37-41.11	12.14	1.9	2.7	0.30	101
7	07/07/84	9.27	39.65	14-54.11	37-44.45	2.99	1.0	0.8	0.24	110
8	14/07/84	23.32	18.64	15-01.46	37-43.45	3.36	0.4	0.3	0.10	126
9	15/07/84	0.21	26.93	15-01.74	37-43.57	3.85	1.1	0.7	0.27	119
10	15/07/84	3.23	2.76	15-00.21	37-46.28	0.38	0.3	0.3	0.11	153
11	15/07/84	21.23	5.04	15-01.75	37-42.92	0.16	0.9	0.9	0.30	144
12	16/07/84	14.13	38.01	15-05.89	37-44.28	1.18	2.3	2.4	0.30	134
13	20/07/84	3.45	55.69	14-51.51	37-46.77	0.93	1.7	1.3	0.22	216
14	22/07/84	8.50	43.04	15-02.18	37-44.97	6.11	1.3	2.8	0.30	72
15	22/07/84	9.47	53.24	15-03.08	37-45.53	4.10	2.2	2.6	0.30	89
16	22/07/84	21.54	52.34	15-03.50	37-44.11	3.44	1.0	0.8	0.21	116
17	24/07/84	5.24	17.07	15-04.77	37-45.42	7.32	1.3	1.7	0.23	82
18	29/07/84	8.54	52.34	15-03.08	37-44.97	3.05	1.9	1.5	0.30	102
19	03/08/84	23.51	33.95	14-55.43	37-50.19	17.39	1.2	1.8	0.13	175
20	03/08/84	23.53	9.68	14-57.92	37-50.65	17.78	2.1	3.8	0.28	175
21	03/08/84	23.56	42.65	14-53.35	37-50.03	27.69	3.2	3.7	0.29	185
22	04/08/84	0.26	1.66	14-53.74	37-51.11	24.32	3.3	3.8	0.29	219
23	12/08/84	0.01	28.16	14-56.39	37-50.04	26.58	2.0	2.8	0.21	168
24	12/08/84	0.37	44.72	14-56.64	37-50.27	29.83	2.4	3.0	0.24	172
25	18/08/84	7.31	0.17	14-58.57	37-43.42	4.03	2.1	1.9	0.30	80
26	28/08/84	4.46	49.84	14-58.47	37-45.88	0.50	0.3	0.3	0.11	98
27	28/08/84	5.56	11.67	14-56.82	37-44.90	10.69	2.3	3.7	0.20	153
28	28/08/84	21.36	51.64	15-00.36	37-44.25	8.10	0.8	1.5	0.11	83
29	28/08/84	23.11	9.01	14-59.93	37-44.25	8.14	1.6	2.6	0.24	83
30	31/08/84	21.06	25.43	14-59.87	37-45.59	3.72	0.9	0.7	0.20	95
31	31/08/84	22.08	11.12	14-58.56	37-46.04	3.01	0.9	1.1	0.14	100
32	27/09/84	16.17	51.07	14-58.57	37-45.36	8.65	1.5	1.8	0.30	92
33	29/09/84	23.07	59.52	14-57.31	37-43.18	11.01	1.1	1.4	0.22	88
34	03/10/84	0.26	58.14	14-59.93	37-44.71	4.88	1.9	1.6	0.30	50
35	14/10/84	4.35	23.26	15-06.96	37-44.18	2.22	1.5	2.1	0.30	153
36	15/10/84	11.03	32.61	15-00.66	37-47.77	0.25	1.1	1.7	0.30	120

among stations as seen from the epicentre (degrees); A.P. = pressure axis; A.T. = tension axis; P.A. and P.B. are the nodal planes from fault plane solutions.

A.P.-strike	A.P.-dip	A.T.-strike	A.T.-dip	P.A.-strike	P.A.-dip	P.A.-slip	P.B.-strike	P.B.-dip	P.B.-slip
282.20	1.80	102.20	88.20	12.16	45.00	90.00	192.16	45.00	89.98
100.00	21.00	6.10	10.10	141.32	67.87	8.13	234.40	82.47	22.33
217.50	58.40	7.80	28.10	288.78	74.40	76.23	66.44	20.70	49.60
278.70	1.70	9.00	31.00	48.85	67.38	21.92	147.65	69.84	24.19
208.10	7.50	29.90	82.50	118.29	52.47	89.70	297.80	37.53	89.61
255.40	81.20	36.90	6.90	120.63	38.37	81.24	311.76	52.15	83.12
254.00	83.90	70.60	6.10	160.15	38.90	89.42	340.89	51.10	89.53
328.00	32.90	97.40	44.50	214.91	83.64	62.23	113.02	28.44	13.46
320.90	0.50	51.00	5.00	186.08	86.88	3.88	95.87	86.12	3.13
159.10	17.10	272.20	51.80	43.75	69.69	54.60	287.72	40.15	32.58
326.00	1.90	217.40	84.10	50.23	43.49	81.89	241.35	47.05	82.38
196.20	52.50	63.30	27.50	314.35	76.36	65.98	196.46	27.42	30.80
181.90	39.10	40.80	43.80	110.62	87.48	69.33	207.25	20.82	7.09
14.40	43.40	244.90	33.90	31.67	28.33	11.10	131.46	84.76	62.11
242.60	9.90	21.10	76.90	343.05	35.91	75.41	145.24	55.41	79.66
317.40	76.50	180.40	9.90	281.42	35.88	74.52	82.55	55.61	79.07
295.00	28.20	103.70	61.30	37.93	17.35	73.81	201.01	73.35	85.02
250.00	42.80	359.70	20.00	44.81	43.73	20.22	299.90	76.18	48.09
93.40	23.30	202.90	37.80	232.08	44.55	12.71	331.20	81.12	46.16
127.20	22.40	249.00	51.90	14.47	73.35	5.61	258.43	34.26	30.59
164.10	44.10	58.00	16.00	190.16	46.62	24.09	297.23	72.74	45.99
74.60	50.90	267.70	38.40	171.82	83.71	83.53	37.79	9.02	44.39
122.90	21.00	250.90	58.10	14.59	69.63	65.55	247.15	31.42	41.89
117.90	38.80	265.60	46.40	12.76	85.98	73.28	269.63	17.18	13.72
86.80	66.90	214.70	14.70	139.12	61.86	70.15	281.69	33.96	57.59
59.60	19.80	281.00	64.50	125.20	28.68	56.27	342.48	66.47	73.10
170.50	65.80	26.50	20.00	285.74	66.23	75.66	138.14	27.54	60.64
86.50	17.00	351.10	17.30	38.69	89.83	24.68	128.77	65.32	0.19
94.40	0.10	184.40	15.40	228.36	79.16	10.94	320.45	79.26	11.04
147.80	20.80	29.40	51.40	81.79	72.52	57.44	196.98	36.50	30.33
201.60	36.50	27.00	53.40	113.90	81.79	87.43	276.44	8.60	72.72
261.80	79.00	6.00	2.70	85.04	43.31	74.37	286.07	48.66	75.75
88.00	24.60	227.90	59.20	343.73	71.73	71.57	210.48	25.72	46.24
28.10	67.00	225.90	22.00	328.03	23.69	74.04	130.68	67.28	83.12
188.30	10.90	84.20	51.90	242.60	46.41	35.76	126.20	64.96	49.55
53.50	56.80	2003.00	29.40	258.35	20.18	45.51	124.75	75.78	75.53

Table II. Focal parameters of earthquakes after the end of the eruption. For explanation of symbols see table I.

No.	Date	h:min (GMT)	Origin	Long(°)	Lat(°)	Depth (km)	ERH	ERZ	RMS	GAP
1	16/10/84	16.13	35.95	14-59.19	37-46.06	3.15	1.30	1.80	0.26	112
2	16/10/84	16.52	36.48	15-3.47	37-45.46	1.37	1.90	1.30	0.30	68
3	16/10/84	17.01	16.14	15-6.05	37-45.71	2.53	2.10	1.50	0.30	71
4	17/10/84	4.14	41.81	15-0.58	37-45.14	3.00	1.30	1.10	0.25	113
5	17/10/84	14.01	38.77	14-50.43	37-44.52	3.32	1.50	1.40	0.30	64
6	17/10/84	16.29	36.29	15-0.50	37-45.44	0.55	2.10	1.90	0.30	98
7	17/10/84	17.58	13.21	15-0.60	37-42.53	7.82	1.90	2.05	0.20	81
8	17/10/84	17.59	7.96	15-0.96	37-44.05	2.94	1.50	1.70	0.29	81
9	17/10/84	18.00	38.01	15-1.19	37-44.31	3.52	1.70	1.40	0.14	124
10	17/10/84	18.02	9.05	15-1.74	37-44.88	1.16	2.30	2.20	0.30	64
11	17/10/84	18.04	48.92	15-1.22	37-43.08	3.77	1.00	0.70	0.17	76
12	17/10/84	18.05	17.93	15-0.04	37-45.89	0.78	1.40	1.20	0.30	59
13	17/10/84	18.11	16.27	14-59.39	37-44.81	2.49	2.10	1.10	0.30	71
14	17/10/84	18.15	0.70	15-1.27	37-42.82	3.96	2.30	2.10	0.30	137
15	17/10/84	18.20	21.45	15-0.46	37-44.48	2.79	1.20	1.10	0.30	66
16	18/10/84	1.28	0.55	15-6.27	37-40.28	29.26	3.10	3.90	0.18	170
17	18/10/84	2.31	8.08	15-0.88	37-44.74	3.38	0.80	0.80	0.16	70
18	18/10/84	4.05	37.64	15-0.63	37-44.80	2.68	1.00	1.20	0.26	65
19	18/10/84	6.28	5.70	15-1.02	37-45.36	2.28	1.30	0.90	0.30	62
20	18/10/84	6.39	40.30	14-59.46	37-43.82	15.12	3.10	4.00	0.30	81
21	18/10/84	11.58	47.56	15-5.51	37-47.19	3.38	1.20	1.00	0.15	139
22	18/10/84	13.50	52.01	15-0.51	37-44.91	3.84	1.10	1.80	0.27	97
23	18/10/84	17.36	0.54	14-48.28	37-35.64	0.50	2.50	2.20	0.25	190
24	19/10/84	1.09	51.75	15-0.84	37-45.41	2.48	1.40	0.80	0.30	62
25	19/10/84	1.13	23.08	15-0.17	37-46.38	0.61	1.20	1.10	0.30	62
26	19/10/84	3.37	54.99	15-1.34	37-44.72	1.26	1.40	0.90	0.30	62
27	19/10/84	3.45	48.59	15-0.52	37-45.01	2.50	1.50	0.80	0.30	93
28	19/10/84	6.51	41.83	15-2.48	37-45.56	3.13	1.20	1.60	0.15	109
29	20/10/84	15.32	15.62	15-10.16	37-44.74	0.77	2.00	1.00	0.17	230
30	20/10/84	16.17	0.77	15-1.75	37-45.42	3.81	1.90	1.30	0.30	109
31	21/10/84	3.43	14.97	15-1.23	37-40.51	0.13	2.50	2.30	0.30	97
32	21/10/84	17.01	21.82	15-2.84	37-44.12	3.98	1.40	1.60	0.29	81
33	22/10/84	2.44	47.01	15-8.12	37-45.44	8.47	1.90	2.40	0.20	181
34	22/10/84	2.48	0.21	14-57.19	37-43.97	10.00	1.70	2.60	0.08	245
35	22/10/84	12.15	54.32	15-2.54	37-49.14	17.79	1.20	4.00	0.09	88
36	22/10/84	15.18	16.76	15-6.19	37-44.15	7.77	1.10	1.70	0.18	114
37	23/10/84	0.14	9.40	14-58.18	37-42.01	1.96	1.00	0.50	0.30	95
38	23/10/84	4.00	39.33	15-2.71	37-44.55	4.04	1.00	1.50	0.16	105
39	23/10/84	4.40	0.21	15-2.07	37-44.99	3.48	1.30	1.00	0.28	189
40	23/10/84	14.19	10.72	14-50.65	37-46.97	2.48	1.60	1.70	0.10	177
41	23/10/84	14.35	4.96	15-5.70	37-43.26	7.78	1.50	2.50	0.25	100
42	23/10/84	14.35	33.35	15-6.00	37-43.34	7.60	2.40	3.00	0.30	107
43	24/10/84	2.27	17.09	15-3.19	37-45.12	6.70	1.10	2.40	0.21	64
44	24/10/84	2.45	14.98	15-0.35	37-46.68	0.19	1.20	1.10	0.30	62
45	24/10/84	6.49	43.81	15-1.71	37-45.42	4.82	1.60	2.10	0.29	83
46	24/10/84	14.01	31.41	15-5.12	37-44.77	2.70	1.60	1.50	0.30	84
47	24/10/84	14.06	52.15	15-4.77	37-44.86	4.95	2.20	1.20	0.30	88
48	24/10/84	17.56	25.73	15-1.61	37-46.00	3.29	1.30	1.60	0.19	86
49	25/10/84	2.41	35.41	15-2.94	37-47.46	3.06	1.00	1.00	0.11	115
50	26/10/84	2.24	22.54	14-59.18	37-45.26	10.59	1.00	3.10	0.20	71
51	26/10/84	5.06	51.75	15-1.74	37-46.47	2.14	1.20	0.70	0.30	66
52	26/10/84	11.37	53.85	15-4.77	37-45.42	0.50	1.40	0.90	0.30	134
53	26/10/84	13.20	34.19	15-5.89	37-44.69	10.45	1.80	3.00	0.24	100
54	26/10/84	13.54	6.87	15-4.98	37-44.57	2.38	0.90	0.50	0.24	83
55	26/10/84	16.04	52.81	15-5.07	37-41.45	3.80	0.90	0.50	0.13	179
56	27/10/84	1.57	18.65	15-4.69	37-44.44	10.56	1.20	1.80	0.21	79
57	27/10/84	6.17	55.70	15-2.09	37-45.70	9.12	1.60	3.00	0.30	56
58	27/10/84	11.10	42.24	15-2.55	37-45.54	9.23	1.30	3.00	0.16	81
59	27/10/84	12.37	11.65	15-3.34	37-45.57	8.33	1.30	2.60	0.26	80
60	27/10/84	14.46	5.90	15-6.50	37-43.88	12.24	2.40	3.70	0.24	122
61	27/10/84	15.21	24.48	14-50.60	37-47.59	31.60	2.40	4.00	0.12	185
62	27/10/84	17.15	55.47	15-0.65	37-46.44	1.80	2.00	1.80	0.30	70
63	28/10/84	1.05	5.86	15-3.50	37-45.10	6.01	0.80	1.50	0.18	65
64	28/10/84	1.37	37.93	15-6.19	37-44.79	8.35	1.00	1.60	0.17	108
65	28/10/84	1.44	0.43	15-3.86	37-45.55	3.86	2.20	1.50	0.30	76
66	28/10/84	15.17	42.53	15-2.91	37-47.38	3.84	1.70	2.20	0.29	76
67	29/10/84	3.27	56.48	15-5.18	37-45.00	0.06	2.60	2.50	0.15	82

A.P.-strike	A.P.-dip.	A.T.-strike	A.T.-dip.	P.A.-strike	P.A.-dip	P.A.-slip	P.B. strike	P.B.-dip	P.B.-slip
239.40	3.70	65.90	86.30	149.84	48.68	89.57	329.19	41.32	89.51
128.00	4.30	36.40	20.20	173.96	72.68	11.51	80.49	79.02	17.66
292.10	28.70	196.40	10.10	330.54	62.36	14.13	67.20	77.51	28.38
271.80	47.20	179.20	2.40	304.21	56.71	35.80	55.81	60.73	39.00
210.90	78.20	339.80	7.40	59.59	38.84	75.47	257.99	52.62	78.58
30.00	36.80	250.00	45.70	60.51	21.64	12.80	318.59	85.31	68.85
210.00	88.20	30.00	1.80	120.00	75.00	90.00	300.00	15.00	90.00
250.00	20.00	30.10	64.60	4.30	28.29	56.85	147.73	66.62	73.60
328.80	79.80	154.10	10.20	63.26	55.19	88.88	245.22	34.82	88.39
210.00	88.20	30.00	1.80	120.00	75.00	90.00	300.00	15.00	90.00
249.70	7.30	69.70	82.70	159.71	42.95	90.00	339.72	47.05	90.00
37.10	21.30	156.60	51.60	283.52	72.69	58.15	167.93	35.80	30.56
210.00	88.20	30.00	1.80	120.00	75.00	90.00	300.00	15.00	90.00
43.40	5.60	248.20	83.80	130.51	39.53	85.93	315.78	50.59	86.65
86.00	62.00	327.20	14.40	86.19	36.88	48.39	218.20	63.34	63.52
138.60	89.00	19.30	0.50	110.17	44.53	88.76	288.44	45.48	88.78
210.00	88.20	30.00	1.80	120.00	75.00	90.00	300.00	15.00	90.00
75.10	6.30	184.90	72.00	183.17	41.43	64.10	330.24	53.47	68.92
199.30	64.40	323.90	15.20	250.31	63.15	67.33	27.56	34.59	52.72
107.50	23.50	9.80	17.00	147.30	60.70	4.93	239.71	85.70	29.39
79.10	51.30	333.70	12.00	215.95	66.10	49.83	100.31	45.68	34.49
215.10	61.00	119.40	3.20	4.69	54.59	53.80	236.32	48.88	50.28
317.50	60.80	77.00	15.40	136.67	36.39	46.43	6.44	64.54	63.07
35.10	71.10	214.20	18.90	124.42	63.93	89.69	303.71	26.07	89.37
71.20	21.00	207.90	62.10	327.07	68.20	71.18	189.62	28.49	51.11
55.40	84.50	270.40	4.50	3.85	40.62	85.21	177.54	49.56	85.90
210.00	22.90	70.10	61.20	133.53	69.61	72.26	270.56	26.56	50.19
46.20	23.10	231.00	66.90	132.57	22.01	85.31	317.62	68.07	88.11
355.80	12.60	264.40	6.40	39.52	76.58	4.44	130.55	85.68	13.46
243.80	66.90	355.50	9.00	62.15	40.51	56.32	283.38	57.28	64.65
32.00	20.00	286.10	36.90	75.12	48.21	14.16	335.57	79.49	42.67
52.70	60.20	313.20	5.40	198.76	56.87	54.31	71.49	47.14	48.21
311.50	40.90	71.20	29.80	8.88	83.07	55.03	108.67	35.57	11.98
84.40	18.40	266.20	71.60	173.55	26.61	88.81	354.88	63.40	89.40
360.00	2.90	251.20	81.00	81.04	42.69	77.35	278.03	48.58	78.58
192.50	62.60	320.20	17.60	246.59	65.58	67.58	21.65	32.68	49.97
58.80	15.40	244.30	74.60	329.95	60.40	88.37	146.66	29.65	87.13
77.20	18.80	177.60	27.90	215.02	56.06	7.09	308.99	84.12	34.14
184.10	37.80	290.50	20.00	233.65	78.91	43.50	334.00	47.50	15.12
234.40	52.80	0.80	24.20	49.63	31.49	31.76	291.80	74.04	62.49
4.60	25.70	180.70	64.30	273.32	70.65	88.36	98.25	19.41	85.35
10.00	12.20	141.30	71.90	268.85	58.46	74.45	116.86	34.81	66.40
236.90	30.80	61.70	59.20	148.67	75.78	87.79	319.75	14.38	81.35
137.30	23.00	243.80	33.90	276.55	47.92	9.20	12.74	83.18	42.45
89.80	35.80	353.30	9.00	226.61	72.34	33.41	125.30	58.36	20.87
30.70	70.40	155.90	11.60	79.10	58.44	71.59	226.64	36.05	62.78
349.90	79.80	247.90	2.10	148.35	47.91	76.48	348.08	43.82	75.49
200.40	25.40	4.90	63.80	304.47	20.21	72.00	105.37	70.82	83.51
196.50	8.80	101.30	30.00	242.98	62.44	16.05	145.39	75.81	28.51
342.70	19.50	122.90	65.30	96.03	28.53	58.12	240.73	66.08	73.98
87.30	14.70	349.90	26.20	36.75	82.42	29.72	131.06	60.57	8.72
303.50	43.00	203.70	10.40	333.57	52.50	26.66	80.56	69.15	40.65
0.60	15.20	236.10	64.30	64.21	34.63	52.66	287.05	63.14	67.27
51.90	60.30	211.10	28.10	128.52	73.67	80.69	278.28	18.74	61.10
87.00	75.70	348.70	2.10	245.36	48.78	70.99	92.95	44.67	69.61
236.00	84.90	141.10	0.50	236.22	44.70	82.75	46.07	45.75	82.88
242.90	66.50	10.00	14.70	76.37	34.12	56.75	294.75	62.03	69.62
323.10	64.00	70.00	8.10	0.58	57.57	60.51	134.06	42.72	52.23
260.10	53.00	27.80	24.70	76.36	30.58	31.88	318.19	74.41	63.35
199.10	77.10	326.60	7.90	44.90	38.14	73.54	245.49	53.68	77.46
247.40	10.10	69.10	79.90	157.66	55.02	89.65	337.04	34.98	89.50
252.10	64.30	55.40	24.70	330.74	70.01	83.09	131.22	21.10	71.70
229.40	25.00	78.20	62.00	294.83	22.65	57.83	149.11	70.97	77.47
201.60	8.20	96.30	61.40	134.07	58.67	57.69	263.50	43.79	48.72
30.00	60.00	250.00	23.90	11.16	26.05	47.99	146.09	70.95	71.88
258.30	3.70	159.70	67.00	188.41	52.76	60.98	325.90	45.88	57.46
215.20	30.30	90.10	44.60	149.78	81.91	59.52	253.21	31.44	15.64

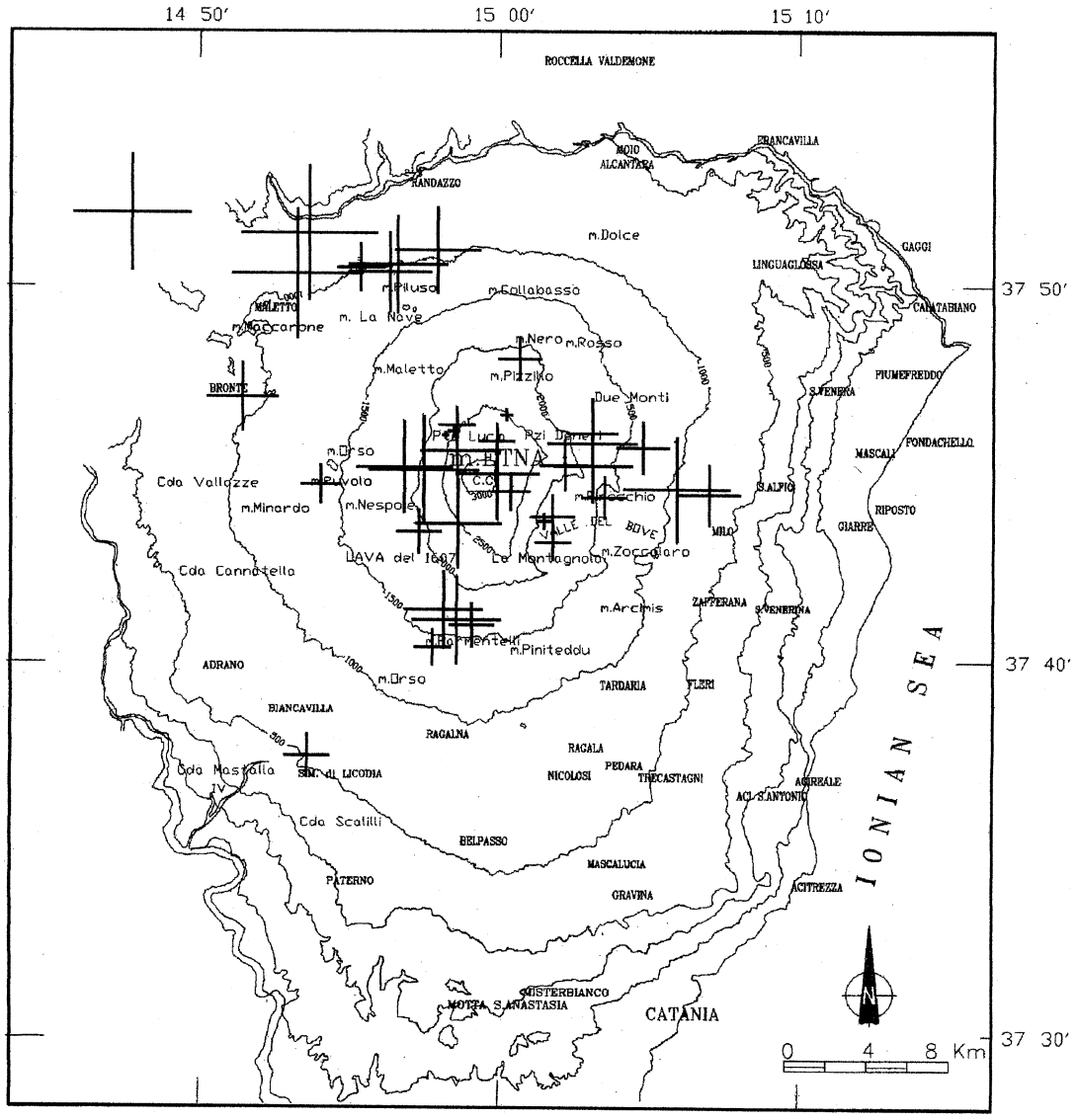

Fig. 2. Epicentral distribution of events from April 15th to October 15th 1984 (eruptive period). Error bars on epicentral determinations are superimposed.

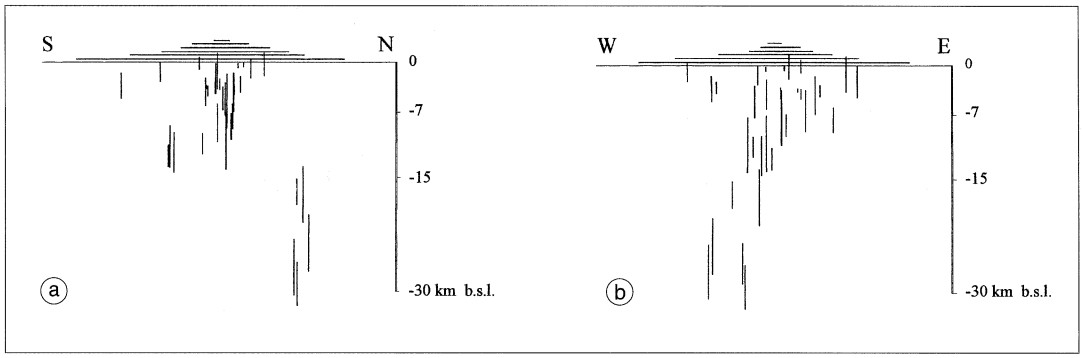

Fig. 3a,b. N-S (a) and E-W (b) vertical sections of hypocentres during eruption; error bars are shown.

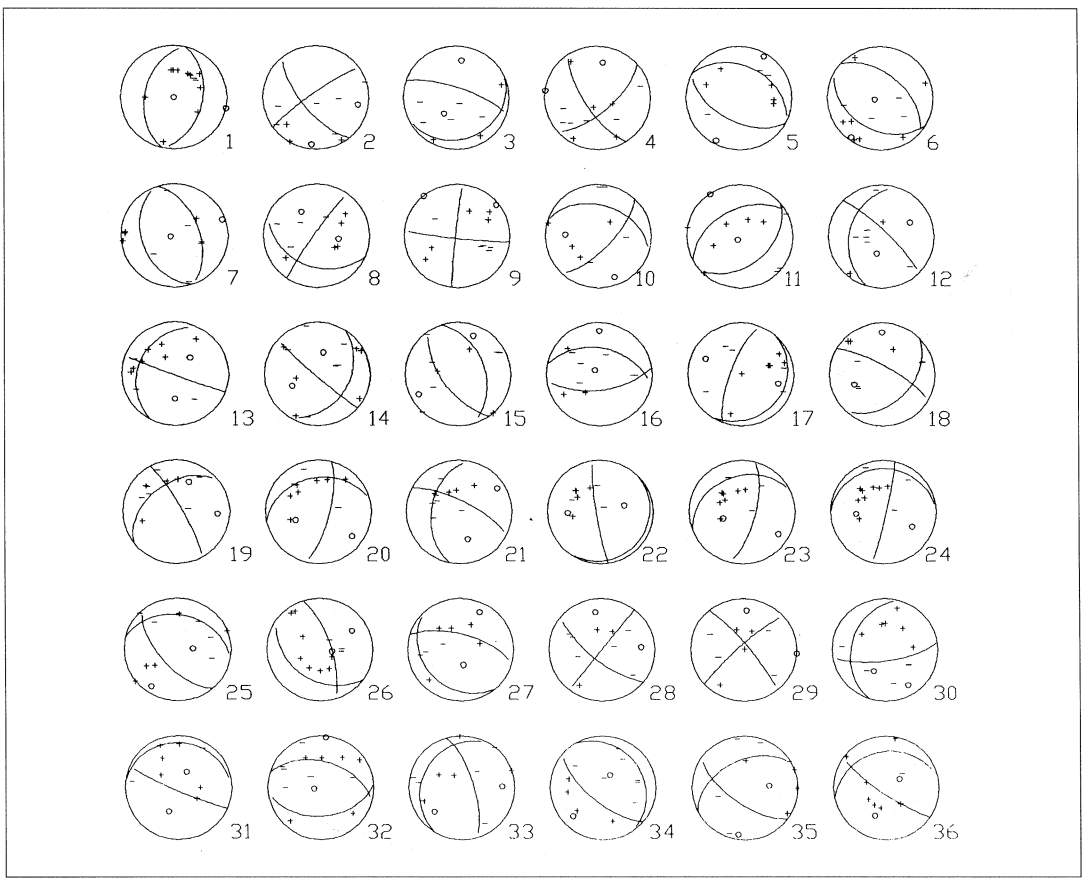

Fig. 4. Fault plane solutions of events (eruptive period) enumerated in the epicentral map of fig. 5; the projections are in the upper hemisphere of Wulff net.

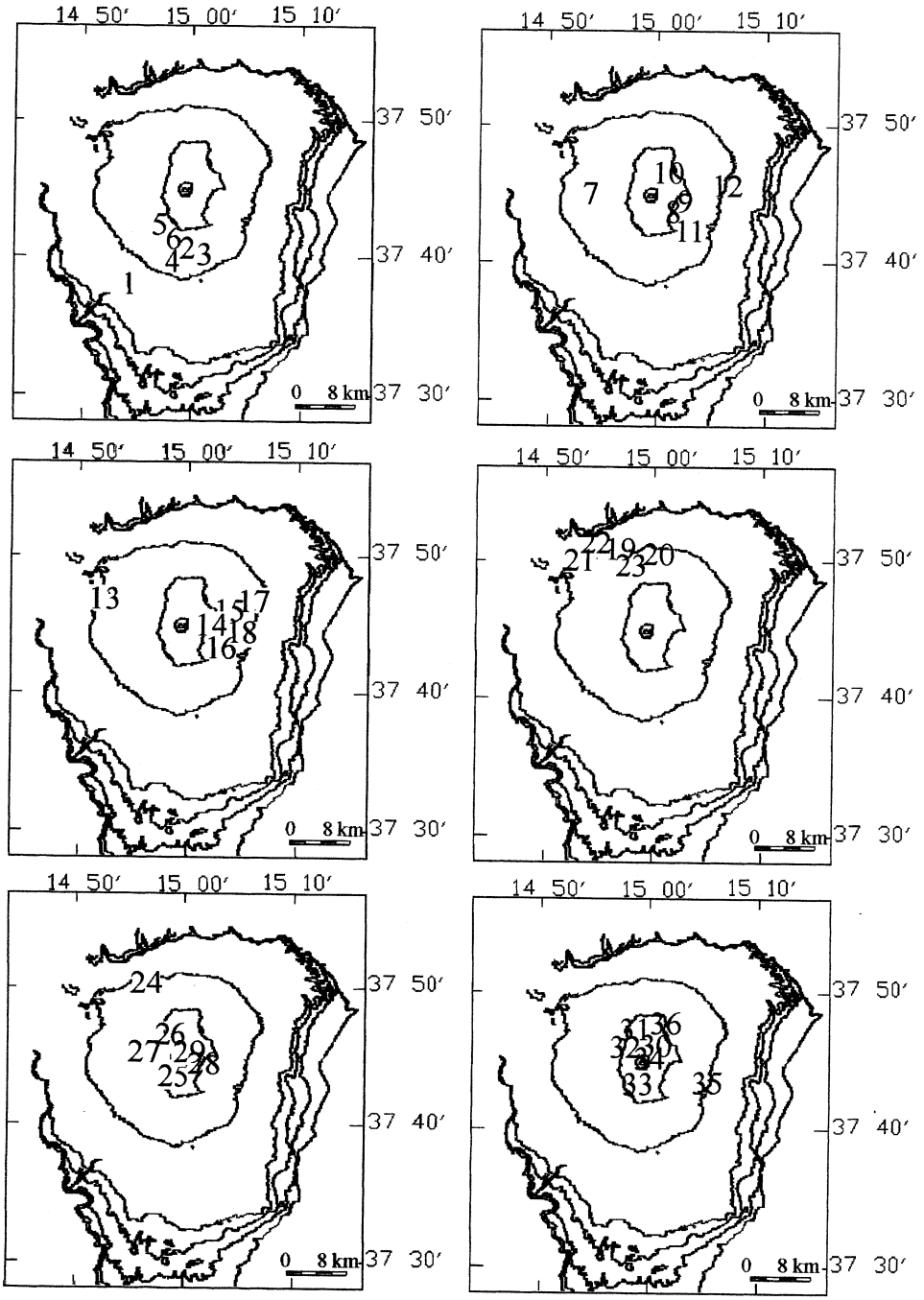

Fig. 5. Maps indicating the epicentres of events analysed in fig. 4 and listed in table I. Several maps are necessary to avoid confusing the numbers.

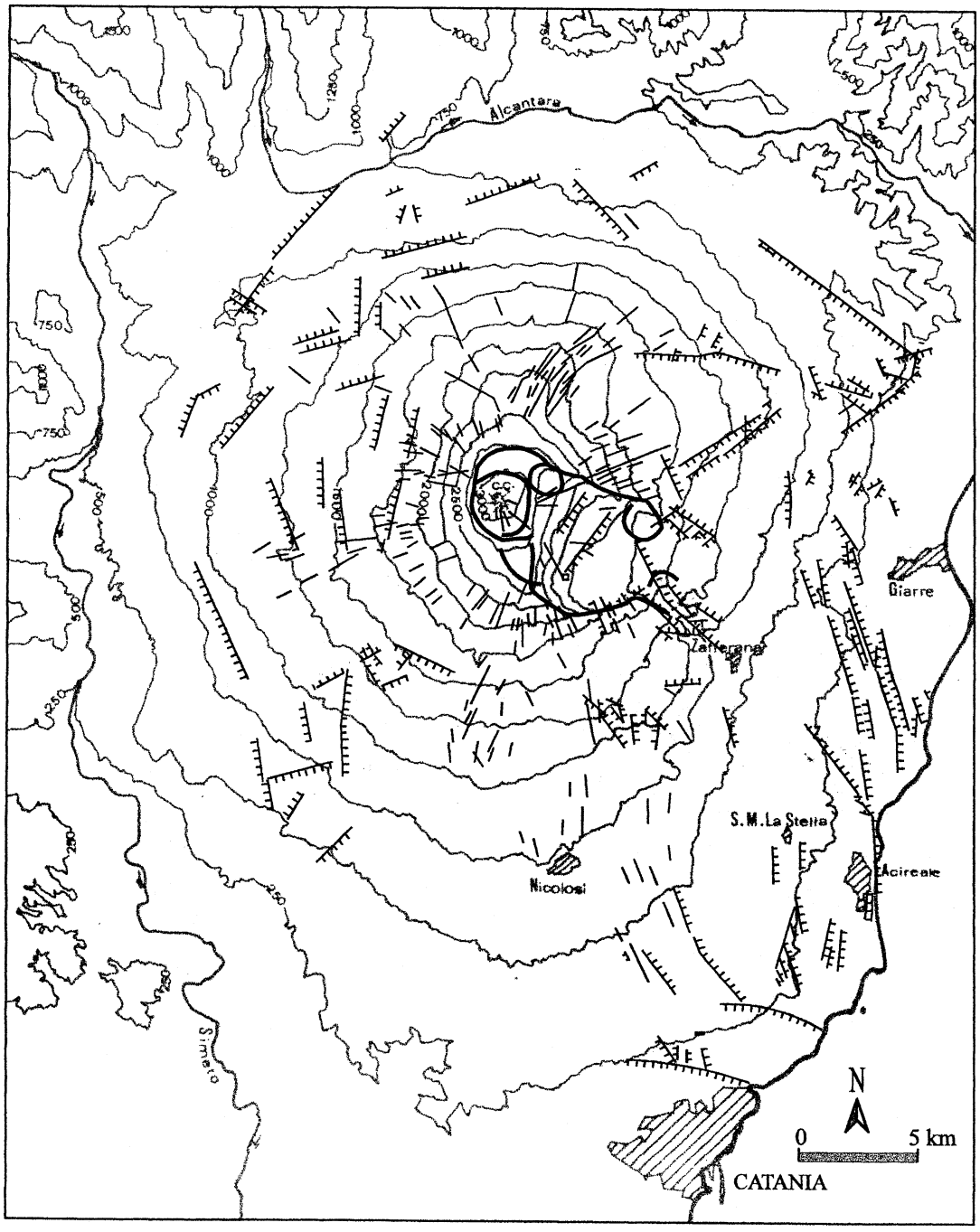

Fig. 6. Structural map of Mt. Etna (from Romano, 1979, modified). This map emphasizes only faults and fractures.

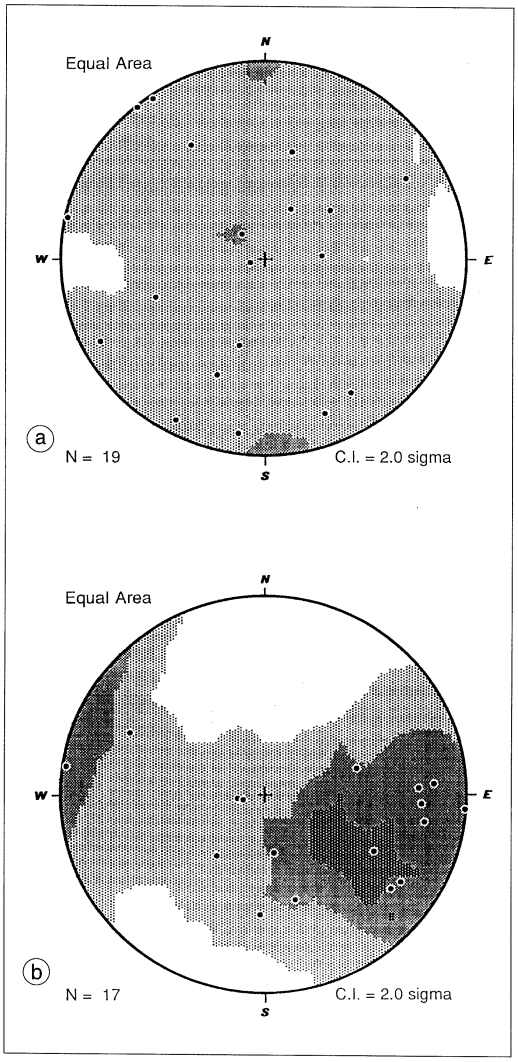

Fig. 7a,b. Diagrams showing the distribution of *P* axes (during eruption) of shallower (a) and deeper (b) earthquakes, respectively. Equal area (Schmidt net) Kamb contour plots. N = No. of axes, C.I. = Contour Interval.

Referring to the volcano-tectonics, epicentres are linked to two main discontinuities: the western rim of «Valle del Bove», where in 1989 and 1991 two extended eruptive fractures oriented NNW-SSE opened, and the fault system called «Timpe della Naca», with a NE-SW trend (1928 eruption) (fig. 10); more pecifically, most of earthquakes are located near the crossing-point of these structures.

Figure 11 shows the focal mechanisms of post eruptive events whose epicentres are enumerated in fig. 12a,b; similar to previous observations, one of two focal planes follows the structural trend of the area where the epicentres are located. The planes are mainly oriented NW-SE, NE-SW and (in minor part) nearly NS and EW for the deeper earthquakes ($H > 7$ km); the shallower ones ($H < 7$ km) are related to fault planes with prevalent NNW-SSE and NW-SE trends, while a minor part shows NE-SW, NNW-SSE, NNE-SSW, nearly NS and nearly EW trends (see also table II).

Some analyzed seismic events have been studied by other researchers considering the effects produced (Patanè and Imposa, 1995).

In particular, the 15th April, 19th June (Benina *et al.*, 1984) and 19th October (Patanè *et al.*, 1994) earthquakes have an hypocentral area aligned NNE-SSW, NNW-SSE and NW-SE, respectively, with a good orientation agreement of the soil fracturation linked to the earthquake, of the tectonic trend of the studied area, and one of the two focal planes.

The seismicity during the month of October, is linked to a tectonic trend oriented according to one of the two focal planes, to which the authors ascribe, even by the last observation, the meaning of the main plane.

The *P* axes of shallower post-eruptive earthquakes (fig. 13a) are mostly concentrated along the NE-SW direction, whereas those regarding the deeper events (fig. 13b) fall mainly into the NNE-SSW trend.

Finally, the plots reported in fig. 14a,b show that during and after the eruption the earthquakes occurred at depths generally less than about 14 km b.s.l.; more in detail, a systematic increase in depth can be noted in fig. 14a for events No. 19-24 (about two months before the end of eruption, see table I); during the post-eruptive period (fig. 14b) most of earthquakes are located at depths less than 7 km b.s.l. until event No. 33 (October 22nd, see table II), while after this date the mean depth of events increases significantly.

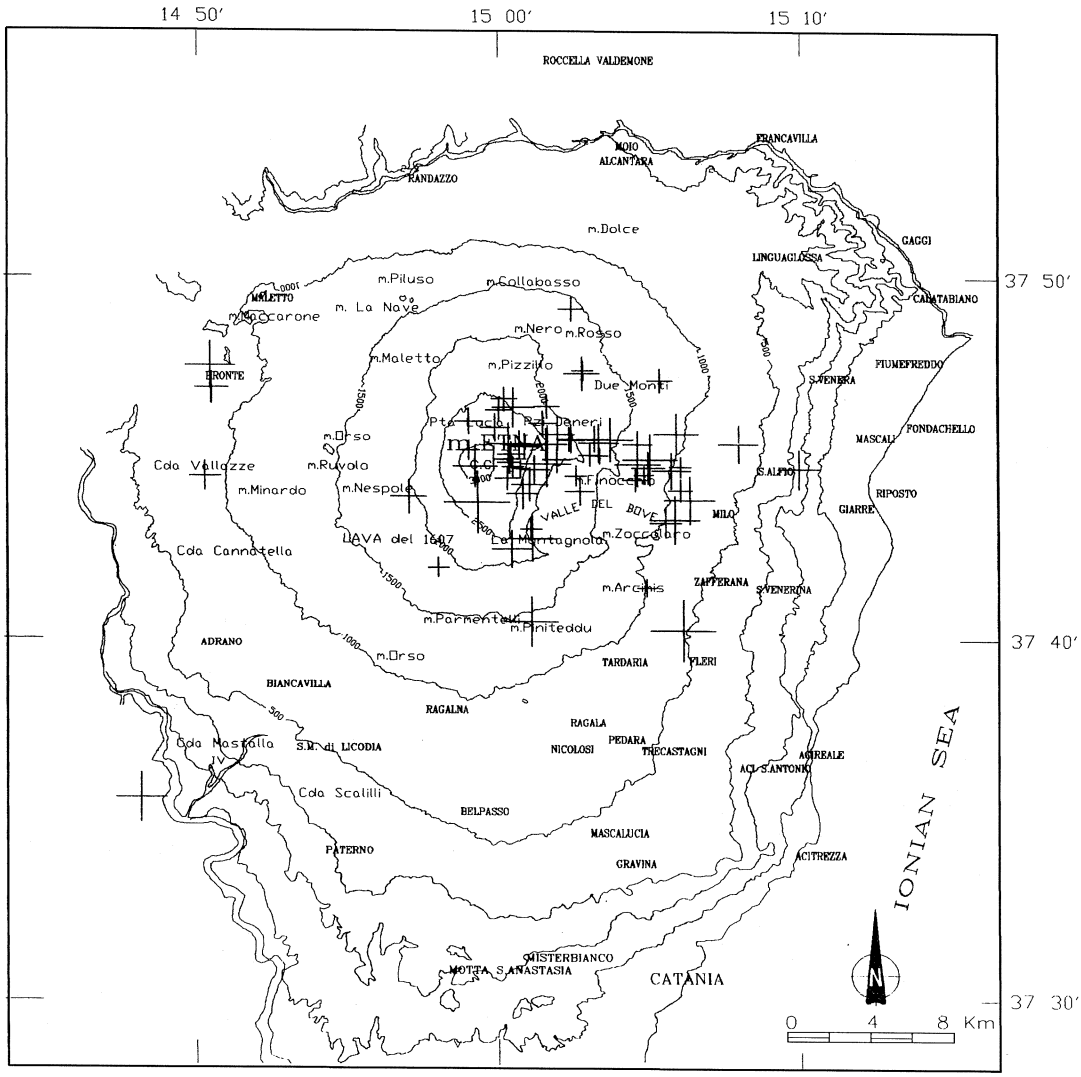

Fig. 8. Epicentral map of earthquakes from October 16th to October 29th 1984 (post-eruptive period). Error bars on epicentral locations are drawn.

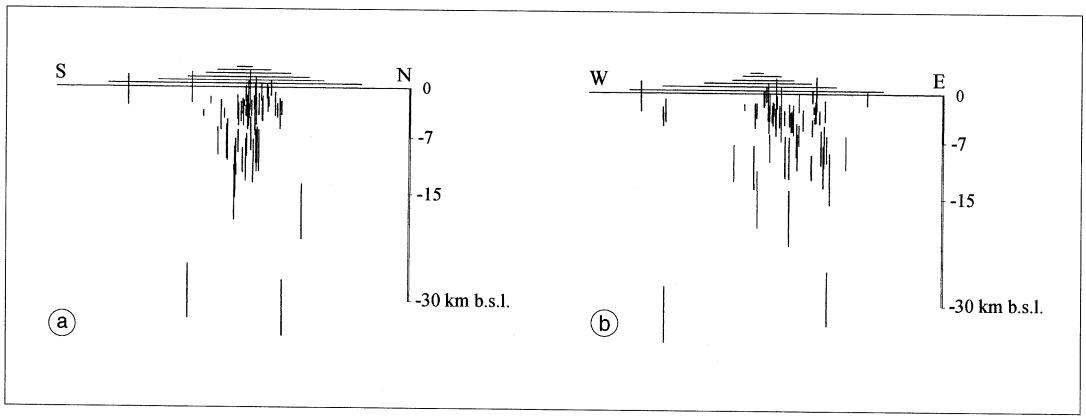

Fig. 9a,b. N-S (a) and E-W (b) vertical sections of hypocentres after eruption; error bars are superimposed.

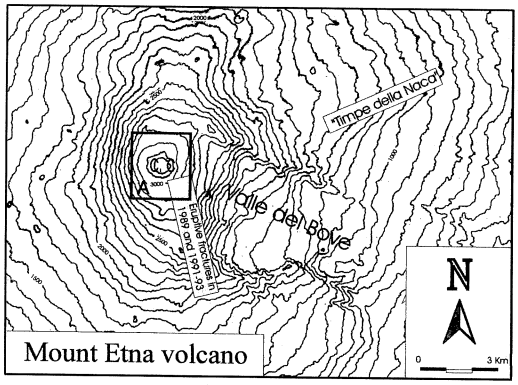

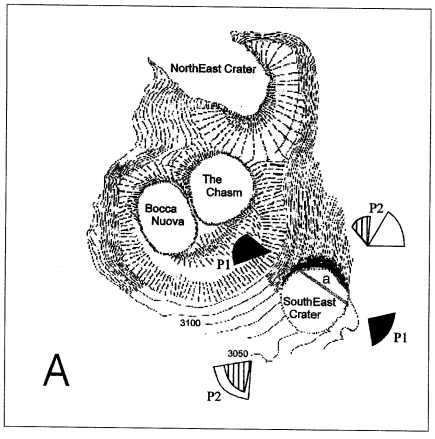

4. Discussion and conclusions

The eruptive event at SE crater, which lasted 130 days, was accompanied and followed by numerous earthquakes with sometimes relatively higher magnitudes ($M \leq 4.2$) (Patanè *et al.*, 1994). The seismic events occurred during the eruption mainly in the western sector and in the upper part of the volcano; after the end of the eruption an increase in seismic activity was observed on the northeastern and eastern flanks, the seismicity at higher altitudes also persisting (Gresta *et al.*, 1987).

The distributions of the *P* axes relative to the deeper earthquakes are clearly different during

Fig. 10. Map of the upper part of Mt. Etna volcano, showing the location of the eruptive fractures on the western side of «Valle del Bove» and «Timpe della Naca». A = Schematic picture of the summit craters; black sectors show the distribution of the *P* axes strike during the eruption (*P*1), white and stippled sectors show the distribution of the *P* axes strike at the end and after the eruption (*P*2); a = eruptive fracture inside SE crater.

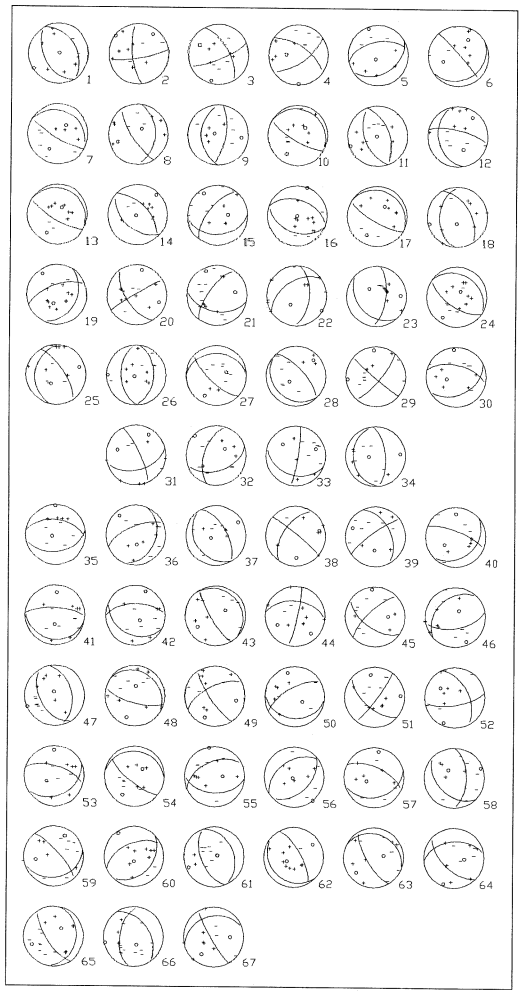

Fig. 11. Fault plane solutions of earthquakes (post-eruptive period) enumerated in the epicentral maps of fig. 12a,b; the projections are in the upper hemisphere of Wulff net.

and after the eruption. The former has average orientation nearly NW-SE, in agreement with the trend of the eruptive fracture which opened inside the SE crater (fig. 10); this trend changes together with the shallow earthquake one at the end and immediately after the eruption, *P* being oriented crossed to the eruptive fracture. Therefore the causes which determined this rotation can be considered responsible for the sharp end of eruption.

A hypothesis about this rotation can be made through some preliminary considerations: the abrupt end of the eruptive event is at the same time as the onset of seismicity, the most violent one in the last thirty years; this seismicity concerned the whole eastern sector of the volcano, gradually passing from north to south (Gresta *et al.*, 1987); the concomitance of these phenomena could be ascribed to the singolar geological and structural frame of the Eastern Sicily.

In fact, passing from south to north, there is a marked thickening of the crust, caused by overlapping of sedimentary and metamorphic formations outcropping just at north of the volcano (Cristofolini *et al.*, 1979), and a remarkable uplifting of the northernmost areas (Mts. Nebrodi and Peloritani). When the crustal thickness remarkably changes about the horizontal direction, a large wide change in potential energy occurs in the crust (Artyushkov, 1973); so the crustal material tends to flow, in this case, from north to south in a transverse direction with respect to the eruptive fracture, and this reduces the crustal thickness inhomogeneities.

The stresses determined by crustal thickness variation and by differential uplifting phenomena can be of thousands of bars (Artyushkov, 1973), and may have caused the temporary closure of the magma uprising fractures, the abrupt stop of the eruptive phenomenon and the following seismicity.

The crust beneath Etna shows a quite different rheology above and below a reference depth of about 7 km. In the shallower level the stresses induce brittle deformations, as confirmed by the presence in the medium of a remarkable number of fractures with various trends (Centamore *et al.*, 1997); this agrees with the observed dispersion of the fault planes and the *P* axes relative to the seismic events located at depth less than 7 km. On the contrary, at deeper levels the seismic activity clearly diminishes.

Moreover, for deeper structures the reaction to the stress field, compared to that of shallower ones, is delayed; this result seems to confirm a visco-elastic rheology for deeper crust beneath the Etnean area.

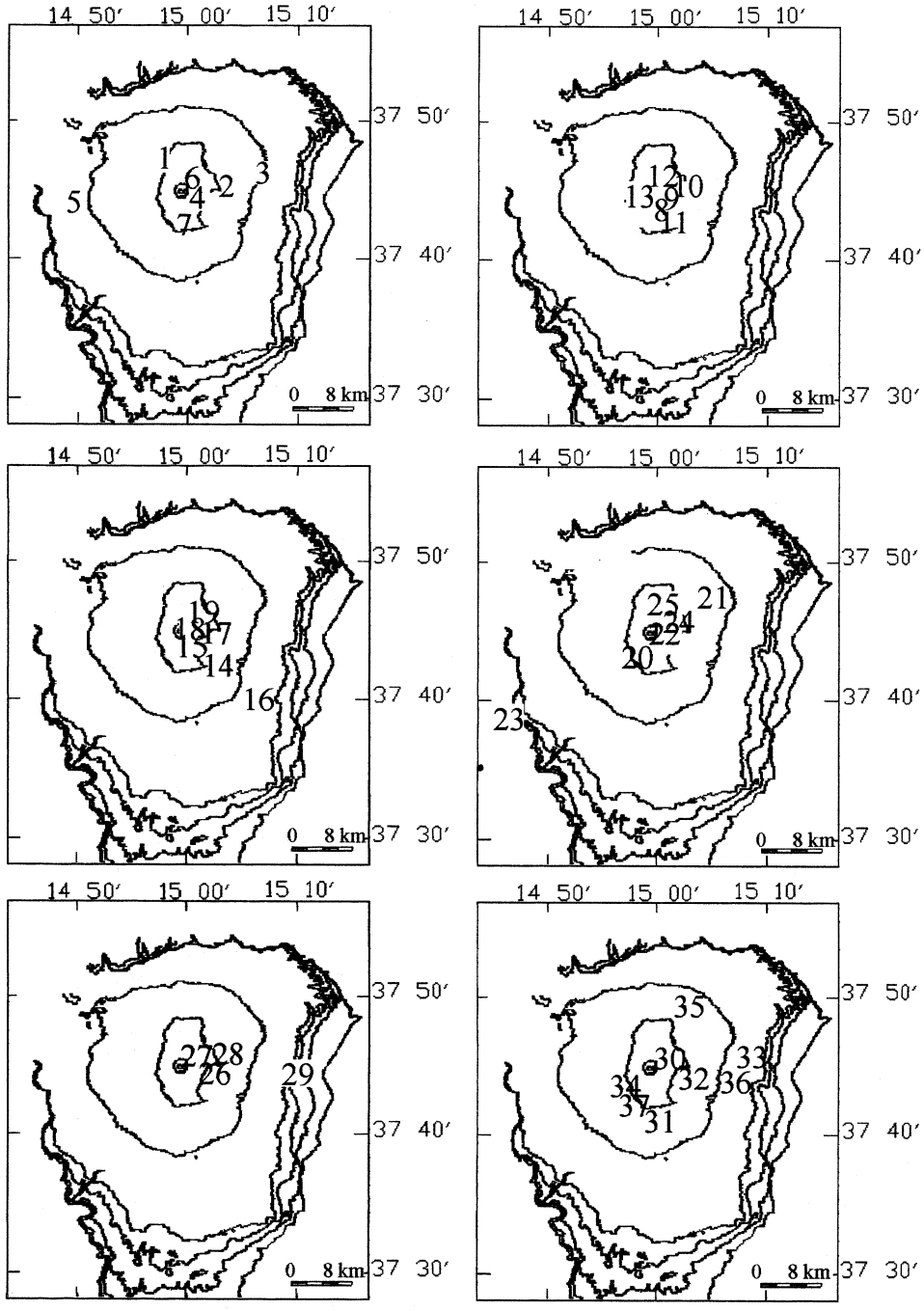

(a)

Fig. 12a,b. Maps indicating the epicentres of events analysed in fig. 11 and listed in table II. Several maps

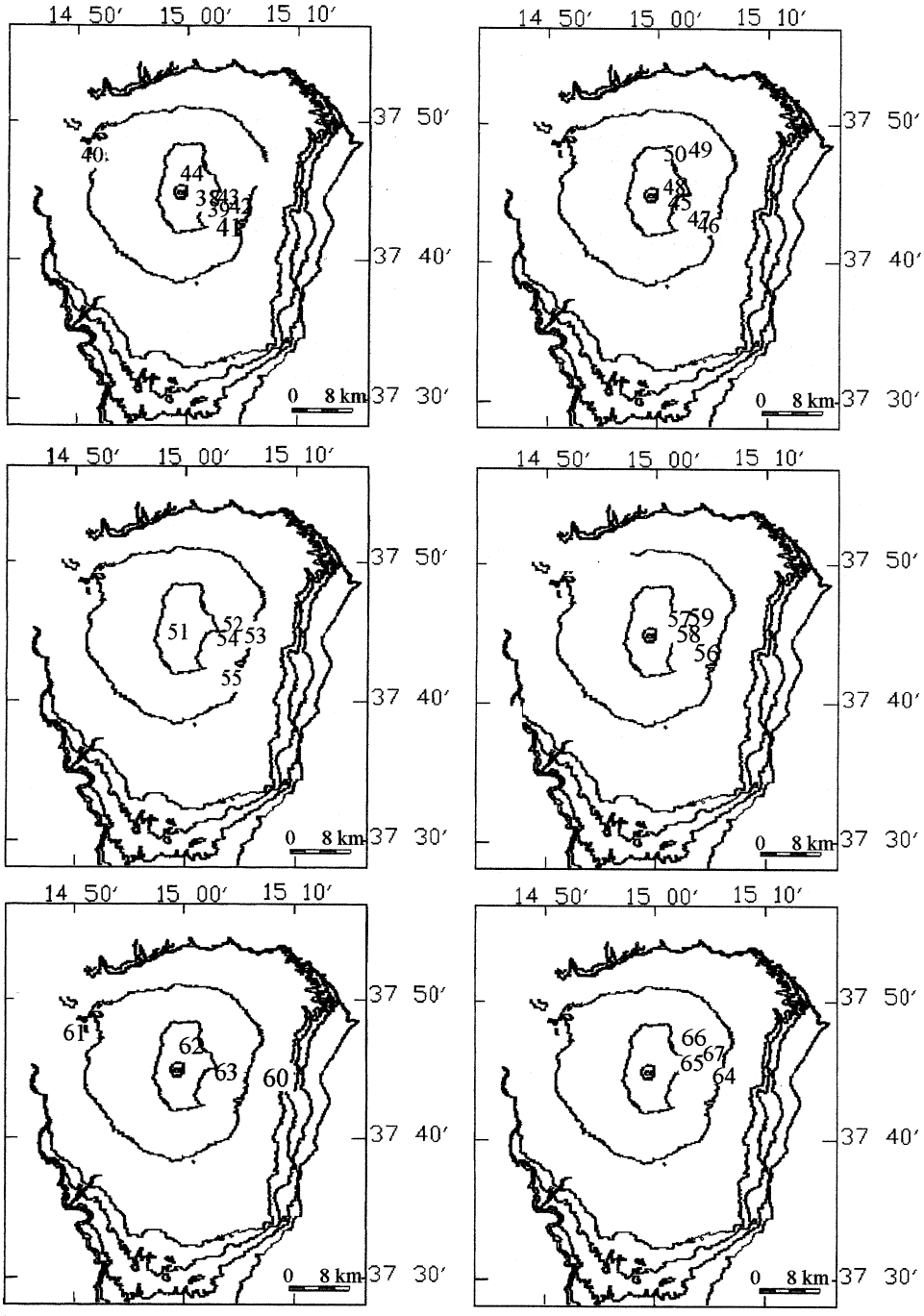

(b)

are necessary to avoid confusing the numbers.

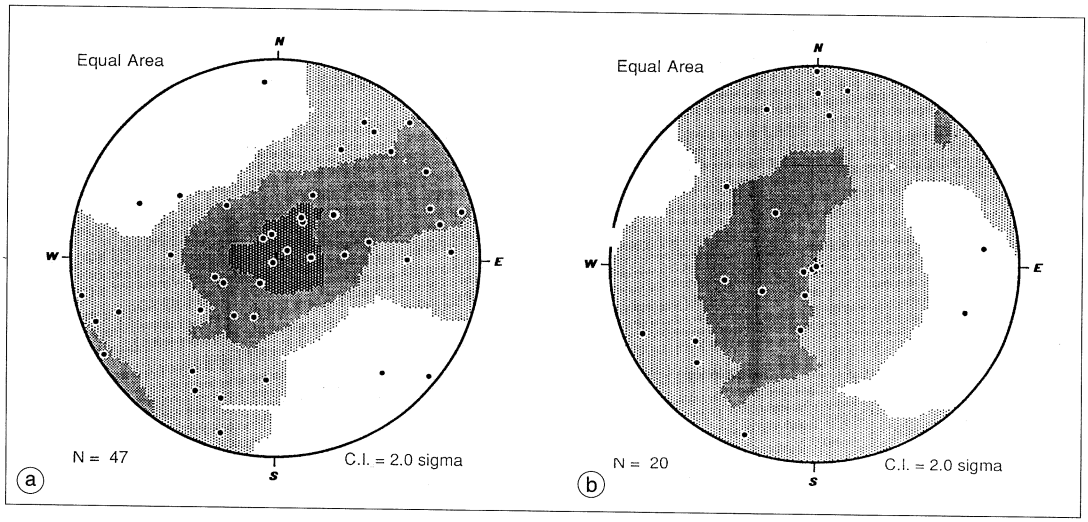

Fig. 13a,b. Graphs indicating the distribution of *P* axes (at the end and after the eruption) of shallower (a) and deeper (b) earthquakes, respectively. Equal area (Schmidt net) Kamb contour plots. N = No. of axes, C.I. = Contour Interval.

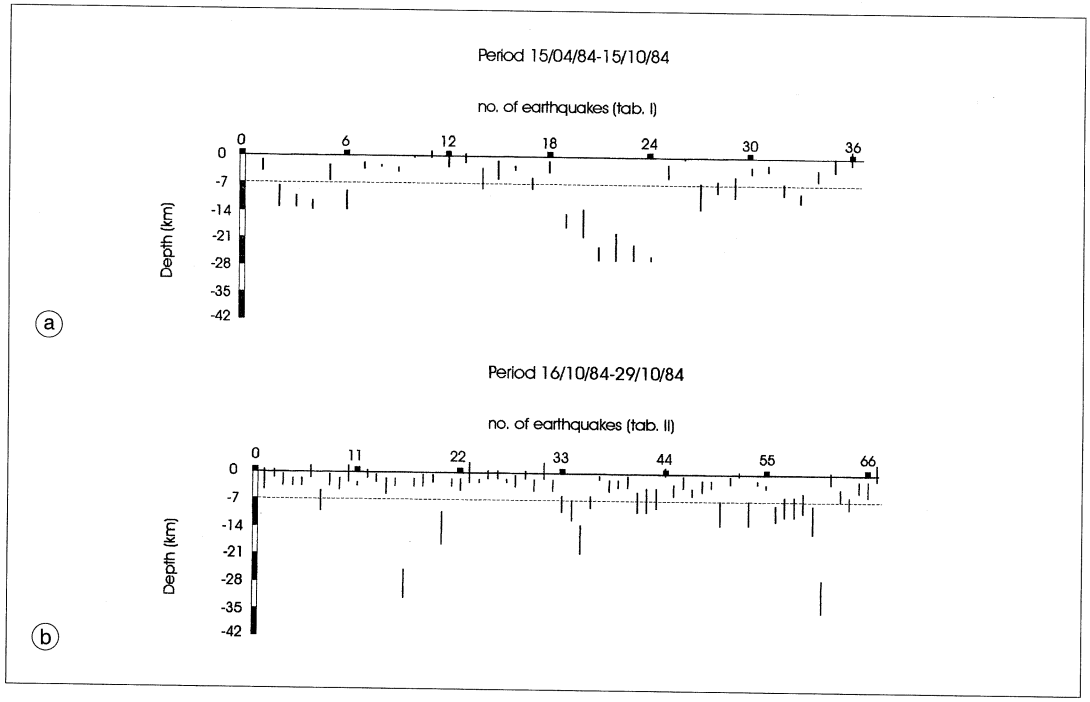

Fig. 14a,b. Diagrams showing the depths of earthquakes in chronological order during (a) and after (b) the eruption, respectively. The reference depth of 7 km is superimposed on each plot.

Finally, the occurrence of deep earthquakes during the eruptive event is probably linked to the uprising of great volumes of magma; this interpretation is supported by the observation of paroxysmal eruptive phenomena in July, August and the first half of September, 1984.

Acknowledgements

This research was carried out by means of grants MURST 40% and 60%.

REFERENCES

ARTYUSHKOV, E.V. (1973): Stresses in the litosphere caused by crustal thickness inhomogeneities, *J. Geophys. Res.*, **78**, 7675-7707.

BENINA, A., S. IMPOSA, S. GRESTA and G. PATANÈ (1984): Studio macrosismico e strumentale di due terremoti tettonici avvenuti sul versante meridionale dell'Etna, in *Atti del 3° Convegno Annuale del GNGTS*, 934-940.

BOTTARI, A., E. LO GIUDICE, G. PATANÈ and C. STURIALE (1975): L'eruzione Etnea del Gennaio-Marzo 1974, *Riv. Min. Sicil.*, **154-156**, 175-198.

CENTAMORE, C., A. MONTALTO and G. PATANÈ (1997): Self-similarity and scaling relations for micro-earthquakes at Mt. Etna volcano (Italy), *Phys. Earth Planet. Inter.*, **103,** 165-167.

COSENTINO, M., G. PATANÈ and P. VILLARI (1979): L'eruzione dell'Etna del Novembre 1978: fenomeni sismici, *P.F. Geodinamica*, Publication No. 4235.

COSENTINO, M., R. CRISTOFOLINI, M. FERRI, G. LOMBARDO, G. PATANÈ, R. ROMANO, A. VIGLIANISI and P. VILLARI (1981): L'eruzione dell'Etna del 17-23 Marzo 1981. Rapporto preliminare, *Rend. Soc. Geol. It.*, **4**, 249-252.

CRISTOFOLINI, R., F. LENTINI, G. PATANÈ and R. RASÀ (1979): Integrazione di dati geologici geofisici e petrologici per la stesura di un profilo crostale in corrispondenza dell'Etna, *Boll. Soc. Geol. It.*, **98**, 239-247.

FERRUCCI, F., R. RASÀ, G. GAUDIOSI, R. AZZARO and S. IMPOSA (1993): Mt. Etna: a model for the 1989 eruption, *J. Volcanol. Geotherm. Res.*, **56**, 35-56.

GLOT, J.P., S. GRESTA, G. PATANÈ and G. POUPINET (1984): Earthquake activity during the 1983 Etna eruption, *Bull. Volcanol.*, **47**, 953-963.

GRESTA, S., J.P. GLOT, G. PATANÈ, G. POUPINET and S. MENZA (1987): The October seismic crisis at Mt. Etna. Part 1: space-time evolution of events, *Ann. Geophys.*, **5B** (6), 671-680.

HIRN, A., A. NERCESSIAN, M. SAPIN, F. FERRUCCI and G. WITTLINGER (1991): Seismic heterogeneity of Mount Etna: structure and activity, *Geophys. J. Int.*, **105**, 139-153.

LEE, W.H. and J.C. LAHR (1975): HYPO71PC (revised): a computer program for determining hypocenter, magnitude and first-motion pattern of local earthquakes, *US Geol. Surv. Open-File Rep.*, 75-311.

LENTINI, F., S. CARBONE and S. CATALANO (1994): Main structural domains of the Central Mediterranean region and their Neogene Tectonic evolution, *Boll. Geofis. Teor. Appl.*, **36** (141-144), 103-125.

PATANÈ, G., S. GRESTA and S. IMPOSA (1984): Seismic activity preceding the 1983 eruption on Mt. Etna, *Bull. Volcanol.*, **47**, 941-952.

PATANÈ, G., S. IMPOSA, S. GRESTA and D. PATANÈ (1986): Rischi derivanti da eventi eruttivi e sismici nell'area etnea, in *Atti V Convegno GNGTS*, 123-126.

PATANÈ, G., A. MONTALTO, S. IMPOSA and S. MENZA (1994): The role of regional tectonics, magma pressure and gravitational spreading in earthquakes of the eastern sector of Mt. Etna volcano (Italy), *J. Volcanol. Geotherm. Res.*, **61**, 253-266.

PATANÈ, G., A. MONTALTO, S. VINCIGUERRA and J.C. TANGUY (1996): A model of the onset of the 1991-1993 eruption of Etna (Italy), *Phys. Earth Planet. Inter.*, **97**, 231-245.

ROMANO, R. (1979): *Geological Map of Mount Etna*, CNR - Roma.

SCARPA, R., G. PATANÈ and G. LOMBARDO (1983): Space-time evolution of seismic activity at Mt. Etna during 1974-1982, *Ann. Geophys.*, **1** (6), 451-462.